

RIS-Aided E2E Multi-Path Uplink Transmission Optimization for 6G Time-Sensitive Services

Zisheng Gong*, Ziyue Xiao*, Liu Cao, Zhaoyu Liu, Dongyu Wei, Lyutianyang Zhang

Abstract—The Access Traffic Steering, Switching, and Splitting (ATSSS) defined in the 3GPP latest Release enables traffic flow over the multiple access paths to achieve the lower-latency End-to-end (E2E) delivery for 6G time-sensitive services. However, the existing E2E multi-path operation often falls short of more stringent QoS requirements for 6G time-sensitive services. This proposes a Reconfigurable Intelligent Surfaces (RIS)-aided E2E multi-path uplink(UL) transmission architecture that explicitly accounts for both radio link latency and N3 backhaul latency, via the coupled designs of the UL traffic-splitting ratio, transmit power, receive combining, and RIS phase shift under practical constraints to achieve the minimum average E2E latency. We develop an alternating optimization framework that updates the above target parameters to be optimized. The simulations were conducted to compare the effectiveness of the proposed E2E optimization framework that lowers the average E2E latency up to 43% for a single user and 15% for the whole system compared with baselines.

Index Terms—ATSSS, E2E, Multi-path, RIS, Latency, 6G.

I. INTRODUCTION

With the rapid growth of Internet-of-Things (IoT) devices towards 6G networks, time-sensitive mobile services have placed tremendous pressure on existing wireless networks [2]. Advanced technologies such as Multi-access Edge Computing (MEC), network slicing, and Ultra-Reliable Low-Latency Communications (URLLC) were leveraged to satisfy the stringent quality of service (QoS) requirements for 5G services. Among these, the End-to-end (E2E) multi-path transmission scheme has emerged as a promising solution to mitigate the E2E multi-path latency for URLLC traffic in dynamic and diverse wireless environments [1].

Traditional cellular networks rely on single E2E path, which however struggle with handling the latency issues. While the E2E multi-path framework utilizes multiple 3GPP accesses (e.g. 5G NR Uu) or non-3GPP accesses (e.g., WLAN 802.11), within the context of Access Traffic Steering, Switching and Splitting (ATSSS) rule [2], [3], to effectively mitigate such issues in the 5G/5G-A era [1]. The authors in [4] investigated

This paper has been presented in part at the IEEE International Conference on Communications in China [1].

*Both authors contributed equally to this work. Zisheng Gong, Ziyue Xiao, Liu Cao, and Zhaoyu Liu are with both City University of Hong Kong (Dongguan), Dongguan, China, and City University of Hong Kong, Hong Kong (e-mail:{72404185, 72405391, liu.cao, 72515198}@cityu-dg.edu.cn). Dongyu Wei is with the Department of Electrical and Computer Engineering, University of Miami, Coral Gables, FL, USA (e-mail: dongyu.wei@miami.edu). Lyutianyang Zhang is with the School of Microelectronics and Communication Engineering, Chongqing University, Chongqing, China (email: zhanglyutianyang@cqu.edu.cn). (Corresponding author: Liu Cao, Lyutianyang Zhang.)

This work was supported by the Youth Innovation Talent Project of Guangdong Provincial Universities (Grant No. 2025KQNCX17).

an optimization problem for traffic scheduling in NR and WLAN aggregation (NWA) for enhanced mobile broadband (eMBB) services. The literature [5] studied an E2E multi-path transmission control protocol (MPTCP) scheduler for latency-sensitive applications. A joint power control and channel allocation scheme was developed in [6] to reduce the interference adaptively. However, 6G time-sensitive services typically are characterized with more stringent QoS requirements, meanwhile, 6G wireless environments with more complex PHY/MAC impairments fundamentally bound the achievable E2E latency mitigation, thereby limiting the effectiveness of existing E2E multi-path schemes.

In this context, Reconfigurable Intelligent Surface (RIS) introduces a novel PHY-layer controllability by actively shaping the wireless environment [7]–[11], enabling the construction of more favorable and stable E2E links. This additional degree of freedom motivates RIS-assisted E2E multi-path optimization, where traffic control across multiple accesses can be jointly designed with propagation-aware link enhancement, offering a viable pathway toward meeting the lower E2E multi-path latency requirements for 6G networks.

Inspired by the aforementioned issues, we propose a RIS-assisted E2E multi-path uplink(UL) transmission architecture that outperforms the existing optimized E2E multi-path approaches. To the best knowledge of authors, this is the first work that integrates both benefits of the RIS and the standardized E2E multi-path architecture that well aligned with the new solution to the lower latency characteristics of 6G time-sensitive services. The key contributions of this paper are summarized as follows.

- We propose a novel E2E multi-path UL transmission architecture with multi-base station (BS) and multi-user (UE) to lower the E2E latency of multi-type time-sensitive traffic with different latency budget requirements;
- We formulate an optimization problem that minimizes the instant E2E latency of the system by jointly optimizing the traffic splitting ratio, UL transmit power, receive combining, and RIS phase shifts, which is further solved by our proposed Alternating Optimization (AO) algorithm.

The remainder of this paper is organized as follows: Section II presents the overall system architecture, Section III provides the problem formulation with the solution, Section IV details the simulation results, and Section V draws the conclusions for this paper.

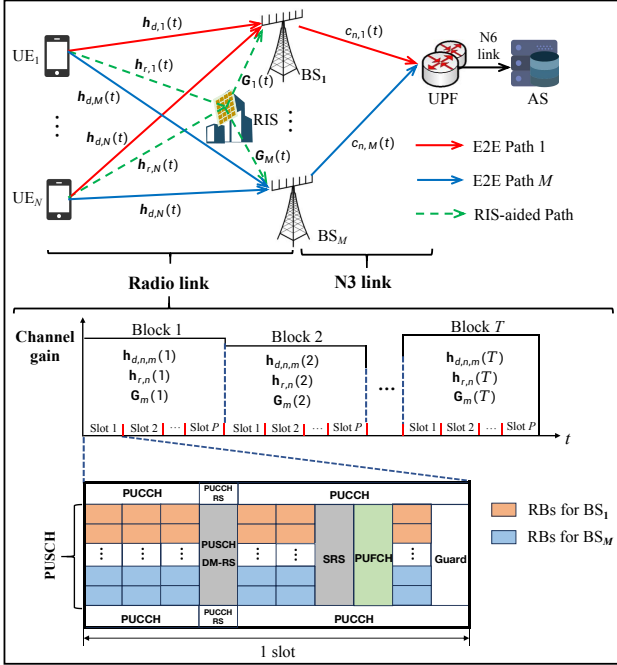


Fig. 1: RIS-aided E2E Multi-path UL Transmission Architecture.

II. SYSTEM ARCHITECTURE

As Fig. 1 shows, we consider an E2E multi-path UL transmission network assisted by an Uniform Planar Array (UPA)-based RIS with $K_x \times K_y$ passive reflecting elements. The system serves $\mathcal{N} = \{1, \dots, N\}$ user equipments (UEs) with each having single transmit (TX) antenna, within the coverage of $\mathcal{M} = \{1, \dots, M\}$ base stations (BSs) of which each has L receive (RX) antennas. Each BS is connected to the User Plane Function (UPF) via an N3 link. Then the UPF is further connected to the Application Server (AS) via an N6 link. Meanwhile, each UE transmits $\mathcal{Q} = \{1, \dots, Q\}$ UL traffic types from the user side to the UPF side, and the traffic of each type is split over the M E2E paths shown in Fig. 1. To minimize the E2E latency that is the sum of the latency over the radio link and the N3 link based on the proposed E2E Multi-path UL transmission architecture, a centralized controller determines: 1) the traffic splitting ratio and the UL transmit power for each UE; 2) the phase-shift for the RIS; and 3) the receive beamforming vectors for each BS.

We consider block-fading channels where the Direct UE-BS UL Channel $\mathbf{h}_{d,n,m}(t)$, UE-RIS UL Channel $\mathbf{h}_{r,n}(t)$, and RIS-BS Channel $\mathbf{G}_m(t)$ between the n th ($n \in \mathcal{N}$) UE and the m th ($m \in \mathcal{M}$) BS in the t th ($t \in \mathcal{T}$) block are assumed to be constant within a block and vary independently over the $\mathcal{T} = \{1, \dots, T\}$ blocks. Each block consists of P consecutive slots with each duration being determined by the 6G numerology. Accordingly, the joint decisions in terms of traffic splitting ratio, UL transmit power, and RIS phase shift are made at the beginning of each block and kept fixed for the whole block. Within each slot, the resource Blocks in the Physical UL Shared Channel (PUSCH) are equally allocated to multiple BSs for the

UL traffic, while the decision information as part of the control information is transmitted in the Physical UL Control Channel (PUCCH). All the relevant feedback to UEs including Channel State Information (CSI) and the decision information (before UEs' UL traffic transmission) is transmitted in the Physical UL Feedback Channel (PUFCH). Note that as all UEs are within the common coverage of the M BSs, each UE will reuse the same RBs allocated for each BS, thereby incurring the inter-user interferences in the UL transmission.

III. SYSTEM MODEL

In this section, we formulate a problem formulation with the algorithm solution for the proposed RIS-aided E2E multi-path framework. The UL channel consists of a direct component and an RIS-assisted cascaded component. Let $\mathbf{h}_{d,n,m}(t) \in \mathbb{C}^{L \times 1}$ denote the direct UL channel from UE $_n$ to BS $_m$, which is given by

$$\mathbf{h}_{d,n,m}(t) = \sqrt{\beta_{d,n,m}} (\eta_{n,m} \mathbf{h}_{n,m}^{\text{LOS}} + \bar{\eta}_{n,m} \mathbf{h}_{n,m}^{\text{NLOS}}), \quad (1)$$

where $\eta_{n,m} = \sqrt{\frac{\kappa_{n,m}}{\kappa_{n,m} + 1}}$ and $\bar{\eta}_{n,m} = \sqrt{\frac{1}{\kappa_{n,m} + 1}}$, $\beta_{d,n,m}$ is the large-scale fading coefficient (pathloss and shadowing), and $\kappa_{n,m} \geq 0$ is the Rician K -factor. The LOS component is modeled by the BS array response vector

$$\mathbf{h}_{n,m}^{\text{LOS}}(t) = e^{j\varphi_{n,m}} \mathbf{a}_{\text{BS}}(\theta_{n,m}^{\text{AoA}}), \quad (2)$$

where $\theta_{n,m}^{\text{AoA}}$ is the AoA at BS $_m$ and $\mathbf{a}_{\text{BS}}(\cdot) \in \mathbb{C}^{L \times 1}$ is the BS array response. For an L -element ULA, it is given by

$$\mathbf{a}_{\text{BS}}(\theta) = \frac{1}{\sqrt{L}} \left[1, e^{-j\frac{2\pi d}{\lambda} \sin \theta}, \dots, e^{-j\frac{2\pi d}{\lambda} (L-1) \sin \theta} \right]^T, \quad (3)$$

where d is the inter-element spacing and λ is the wavelength. The NLOS component accounts for rich scattering and spatial correlation

$$\mathbf{h}_{n,m}^{\text{NLOS}} = (\mathbf{R}_{n,m}^{\text{BS}})^{\frac{1}{2}} \mathbf{g}_{n,m}, \quad (4)$$

where $\mathbf{g}_{n,m} \sim \mathcal{CN}(\mathbf{0}, \mathbf{I}_L)$ and $\mathbf{R}_{n,m}^{\text{BS}} \in \mathbb{C}^{L \times L}$ is the receive correlation matrix at BS $_m$.

Let $\mathbf{h}_{r,n}(t) \in \mathbb{C}^{K_y \times 1}$ denote the UL channel from UE $_n$ to the RIS. A geometry-based finite-path model is adopted as

$$\mathbf{h}_{r,n}(t) = \sqrt{\beta_{r,n}} \sum_{s=1}^{S_r} \xi_{n,s} \mathbf{a}_{\text{RIS}}(\varphi_{n,s}^{\text{AoA}}, \theta_{n,s}^{\text{AoA}}), \quad (5)$$

where $\beta_{r,n}$ is the large-scale fading on the UE-RIS link, S_r is the number of resolvable paths, $\xi_{n,s}$ is the complex gain of path s , and $\mathbf{a}_{\text{RIS}}(\cdot) \in \mathbb{C}^{K_y \times 1}$ is the RIS array response. For a $K_x \times K_y$ UPA, the RIS array response is given by

$$\mathbf{a}_{\text{RIS}}(\varphi, \theta) = \mathbf{a}_x(\varphi, \theta) \otimes \mathbf{a}_y(\varphi, \theta), \quad (6)$$

with

$$\mathbf{a}_x(\varphi, \theta) = \frac{1}{\sqrt{K_x}} \left[1, e^{-j\frac{2\pi d_x}{\lambda} u_x}, \dots, e^{-j\frac{2\pi d_x}{\lambda} (K_x-1) u_x} \right]^T, \quad (7)$$

$$\mathbf{a}_y(\varphi, \theta) = \frac{1}{\sqrt{K_y}} \left[1, e^{-j\frac{2\pi d_y}{\lambda} u_y}, \dots, e^{-j\frac{2\pi d_y}{\lambda} (K_y-1) u_y} \right]^T, \quad (8)$$

where $u_x = \sin \theta \cos \varphi$ and $u_y = \sin \theta \sin \varphi$, d_x and d_y are the inter-element spacings along the x - and y -axes of the RIS, respectively.

Let $\mathbf{G}_m(t) \in \mathbb{C}^{L \times K}$ denote the channel from the RIS to BS_m . We adopt a finite-path geometric channel model as

$$\mathbf{G}_m(t) = \sqrt{\beta_{G,m}} \sum_{s=1}^{S_G} \rho_{m,s} \mathbf{a}_{\text{BS}} \left(\vartheta_{m,s}^{\text{AoA}} \right) \mathbf{a}_{\text{RIS}}^H \left(\varphi_{m,s}^{\text{AoD}}, \theta_{m,s}^{\text{AoD}} \right), \quad (9)$$

where $\beta_{G,m}$ is the large-scale fading on the RIS-BS link, S_G is the number of paths, $\rho_{m,s}$ is the complex gain, and $\vartheta_{m,s}^{\text{AoA}}$ is the AoA at BS_m . $\varphi_{m,s}^{\text{AoD}}$ and $\theta_{m,s}^{\text{AoD}}$ are the pitch and azimuth AoD from the RIS, respectively.

The RIS is modeled by a diagonal phase-shift matrix as

$$\Phi(t) = \text{diag}(\phi_1(t), \dots, \phi_K(t)), \quad (10)$$

where $\phi_k(t) = e^{j\theta_k(t)}$ denotes the reflection coefficient of the k -th element. Since the RIS is passive, it satisfies the unit-modulus constraint $|\phi_k(t)| = 1, \forall k$. Accordingly, the RIS-aided effective UL channel from UE_n to BS_m is

$$\mathbf{h}_{n,m}(t) = \mathbf{h}_{d,n,m}(t) + \mathbf{G}_m(t) \Phi(t) \mathbf{h}_{r,n}(t). \quad (11)$$

Let $x_{n,m}(t)$ denote the unit-power UL stream from UE_n intended for BS_m with $\mathbb{E}[|x_{n,m}(t)|^2] = 1$, and let $p_{n,m}(t) \geq 0$ be the corresponding transmit power allocated to link (n, m) . Then the received signal at BS_m is

$$\mathbf{y}_m(t) = \sum_{n=1}^N \sqrt{p_{n,m}(t)} \mathbf{h}_{n,m}(t) x_{n,m}(t) + \mathbf{z}_m(t), \quad (12)$$

where $\mathbf{z}_m(t) \sim \mathcal{CN}(\mathbf{0}, \sigma^2 \mathbf{I}_L)$ is the receiver noise. Since each UE transmits the sub-flow destined for BS_m on orthogonal time-frequency resources associated with that BS, as is shown in Fig. 1, the symbol $x_{n,m}(t)$ is only observed on BS_m 's resource, and there is no intra-UE cross-path interference.

For each BS_m , define the receive combining matrix $\mathbf{W}_m(t) \triangleq [\mathbf{w}_{m,1}(t), \dots, \mathbf{w}_{m,N}(t)] \in \mathbb{C}^{L \times N}$. Let $\mathbf{W}(t) \triangleq \{\mathbf{W}_m(t)\}_{m \in \mathcal{M}}$ denote the collection of all receive combiners. In this work, $\mathbf{W}(t)$ is updated using the Minimum Mean Square Error (MMSE) receive combiner based on the current $\alpha_{n,m,q}(t)$, $p_{n,m}(t)$, and $\Phi(t)$. Particularly, BS_m uses $\mathbf{w}_{m,n}(t)$ to decode UE_n 's uplink stream as follows:

$$\hat{x}_{n,m}(t) = \mathbf{w}_{m,n}^H(t) \mathbf{y}_m(t). \quad (13)$$

The SINR at the BS_m from the UE_n is

$$\gamma_{n,m}(t) = \frac{p_{n,m}(t) |\mathbf{w}_{m,n}^H(t) \mathbf{h}_{n,m}(t)|^2}{\sum_{j \neq n} p_{j,m}(t) |\mathbf{w}_{m,n}^H(t) \mathbf{h}_{j,m}(t)|^2 + \sigma^2 \|\mathbf{w}_{m,n}(t)\|^2}, \quad (14)$$

Accordingly, the achievable UL rate (bits/second) from the UE_n to the BS_m is

$$R_{n,m}(t) = B_m \log_2 (1 + \gamma_{n,m}(t)). \quad (15)$$

where B_m denotes the bandwidth of the UL resource associated with BS_m . According to Fig. 1, the latency on each E2E path includes the latency over the radio link and the N3 link. Suppose the number of arrived packets of traffic type

q at UE_n in block t is a random variable $\lambda_{n,q}(t)$ following a Poisson distribution with mean $\mathbb{E}[\lambda_{n,q}(t)] = \bar{\lambda}_{n,q}$. Each packet of traffic type q has a fixed size of M_q bits, and all packets with the same type share the same size. Meanwhile, let $n_{n,q}(t)$ denote the number of queueing packets of type q at UE_n at the beginning of block t , which also follows a Poisson distribution with mean $\mathbb{E}[n_{n,q}(t)] = \bar{n}_{n,q}$. We denote the fraction of type q UL traffic from UE_n routed to BS_m is $\alpha_{n,m,q}(t)$, satisfying $0 \leq \alpha_{n,m,q}(t) \leq 1$ and $\sum_{m=1}^M \alpha_{n,m,q}(t) = 1, \forall n \in \mathcal{N}, \forall q \in \mathcal{Q}$. Therefore, the corresponding propagation latency for traffic type q over the radio link from UE_n to BS_m is obtained by

$$\tau_{n,m,q}^{\text{UL}}(t) = \frac{\alpha_{n,m,q}(t) (\lambda_{n,q}(t) + n_{n,q}(t)) M_q}{R_{n,m}(t)}, \quad (16)$$

The backhaul latency for traffic type q over N3 link from BS_m to UPF is given by

$$\tau_{n,m,q}^{\text{BH}}(t) = \frac{\alpha_{n,m,q}(t) (\lambda_{n,q}(t) + n_{n,q}(t)) M_q}{c_{n,m,q}(t)}, \quad (17)$$

where $c_{n,m,q}(t)$ follows a uniform distribution based on the QoS flow characteristics. As a result, the estimated instant E2E latency for traffic $q \in \mathcal{Q}$ via the E2E path m of the UE n at the block t is

$$u_{n,m,q}(t) = \tau_{n,m,q}^{\text{UL}}(t) + \tau_{n,m,q}^{\text{BH}}(t). \quad (18)$$

Our objective is to minimize the instant E2E UL latency per block of all UEs with all traffic types based on the proposed architecture in Fig. 1. Accordingly, we formulate a joint optimization problem that minimizes the E2E latency per block in terms of UE configurations including traffic splitting and transmit power, the RIS configuration, and the BS configuration as below:

Problem 1 (RIS-aided E2E Multi-path UL Optimization).

$$\begin{aligned} & \underset{\alpha_{n,m,q}(t), p_{n,m}(t), \mathbf{W}(t), \Phi(t)}{\text{argmin}} \quad f = \sum_{n \in \mathcal{N}} \sum_{q \in \mathcal{Q}} \max_{m \in \mathcal{M}} u_{n,m,q}(t) \\ & \text{s.t.} \quad \text{C1: } 0 \leq \alpha_{n,m,q}(t) \leq 1, n \in \mathcal{N}, m \in \mathcal{M}, q \in \mathcal{Q}, \\ & \quad \text{C2: } \sum_{m=1}^M \alpha_{n,m,q}(t) = 1, n \in \mathcal{N}, q \in \mathcal{Q}, \\ & \quad \text{C3: } 0 \leq p_{n,m}(t) \leq P_n^{\text{tot}}, n \in \mathcal{N}, m \in \mathcal{M}, \\ & \quad \text{C4: } \sum_{m=1}^M p_{n,m}(t) = P_n^{\text{tot}}, n \in \mathcal{N}, \\ & \quad \text{C5: } \|\mathbf{w}_{m,n}(t)\|^2 \leq 1, m \in \mathcal{M}, n \in \mathcal{N}, \\ & \quad \text{C6: } \Phi(t) = \text{diag}(e^{j\theta_1(t)}, \dots, e^{j\theta_K(t)}), \\ & \quad |\phi_k(t)| = 1, \forall k \in \{1, \dots, K\}, \\ & \quad \text{C7: } 0 \leq u_{n,m,q}(t) \leq T_q^{\text{max}}, q \in \mathcal{Q}, \end{aligned} \quad (19)$$

where P_n^{tot} is the total UL transmit power for UE_n . T_q^{max} is the latency budget of traffic type q .

Remark 1. Problem 1 is non-convex due to the coupled SINR and UL rate expressions in Eq. (14)–(15) and the unit-modulus RIS constraint in C6. Specifically, the SINR in Eq. (14) couples the receive combining vectors $\mathbf{W}(t)$, the RIS phase-shift matrix $\Phi(t)$, and the UL transmit power $\{p_{n,m}(t)\}$

Algorithm 1: Alternating Optimization (AO) for Problem 1

Input: $R_{\max}, I_{\max}, \epsilon_{AO}, \epsilon_{SCA}$;
Output: $\mathbf{W}^*, \alpha^*, p^*, \Phi^*$;
Init: Feasible (α^0, p^0, Φ^0) ; $\mathbf{W}^0 \leftarrow \text{MMSE}(p^0, \Phi^0)$;
 $f^0 \leftarrow f(\alpha^0, p^0, \mathbf{W}^0, \Phi^0)$
for $r = 0$ **to** $R_{\max} - 1$ **do**
 $\mathbf{W}^{r+1} \leftarrow \text{MMSE}(p^r, \Phi^r)$;
 for $i = 0$ **to** $I_{\max} - 1$ **do**
 $(\alpha^{i+1}, p^{i+1}) \leftarrow \text{SCA}(\mathbf{W}^{r+1}, \Phi^r, \alpha^i, p^i)$;
 if $\frac{\|\alpha^{i+1} - \alpha^i\|_2 + \|p^{i+1} - p^i\|_2}{\max\{1, \|\alpha^i\|_2 + \|p^i\|_2\}} \leq \epsilon_{SCA}$ **then**
 break;
 $(\alpha^{r+1}, p^{r+1}) \leftarrow (\alpha^{i+1}, p^{i+1})$;
 $\mathbf{V}^{r+1} \leftarrow \text{SDR}(\mathbf{W}^{r+1}, \alpha^{r+1}, p^{r+1})$;
 $\tilde{\mathbf{v}}^{r+1} \leftarrow \text{Gaussian-Randomization}(\mathbf{V}^{r+1})$;
 $\mathbf{v}^{r+1} \leftarrow \tilde{\mathbf{v}}^{r+1} \leftarrow \text{entry-wise projection}$;
 $\Phi^{r+1} \leftarrow \text{diag}(e^{j\angle \mathbf{v}^{r+1}}) \leftarrow \text{unit-modulus projection}$;
 $f^{r+1} \leftarrow f(\alpha^{r+1}, p^{r+1}, \mathbf{w}^{r+1}, \Phi^{r+1})$;
 if $\frac{|f^{r+1} - f^r|}{\max\{1, |f^r|\}} \leq \epsilon_{AO}$ **then**
 break;
return $\{\mathbf{w}^{r+1}, \alpha^{r+1}, p^{r+1}, \Phi^{r+1}\}$;

through multiplicative terms in both the desired signal and interference components. Meanwhile, the achievable UL rate in Eq. (15) introduces a nonlinear mapping from SINR to the UL rate, and the E2E latency further contains inverse-rate type terms (e.g., traffic amount divided by achievable rate) that strengthens the non-convexity. Finally, the constraint $|\phi_k(t)| = 1$ in C6 renders the feasible set of RIS coefficients non-convex.

Motivated by Remark 1, we propose an alternating optimization (AO) framework that iteratively updates $\mathbf{W}(t)$, $\alpha(t)$, $p(t)$, and $\Phi(t)$ to solve Problem 1. For notational convenience, we omit the index of block t , UE _{n} , BS _{m} , traffic type q and unless otherwise stated. Specifically, \mathbf{W} is updated by the MMSE receive combiner, (α, p) is updated by solving an Successive Convex Approximation (SCA)-based convex subproblem with at most I_{\max} inner iterations (tolerance ϵ_{SCA}), and Φ is updated via the Semidefinite Program (SDP) optimization. The Semidefinite Relaxation (SDR) step leads to a SDP, which can be efficiently solved by standard convex solvers. The AO iterations stop when the objective improvement between two successive iterations is below a prescribed threshold ϵ_{AO} , or when the maximum number of AO iterations R_{\max} is reached. The overall procedure is summarized in Algorithm 1 [7], [12], [13]. As a result, the average E2E UL latency over all T blocks per UE shown in Fig.1 is expressed as

$$\bar{U} = \frac{1}{NT} \sum_{t \in \mathcal{T}} f(\alpha^*, p^*, \mathbf{W}^*, \Phi^*, t), \quad (20)$$

where T should be large enough to estimate the converged one.

IV. SIMULATION

In this section, simulations are conducted in Matlab with CVX Toolbox to quantify the performance gain of the proposed E2E multi-path architecture with algorithm. We consider a

scenario of 3 BSs and 3 UEs, where the 3 BSs are placed in a triangular layout, forming spatially diverse access paths for the UEs, and each UE is within the coverage of the 3 BSs thereby the traffic can be split among the 3 E2E paths. The RIS is implemented as a 10×10 UPA with half-wavelength spacing, and the RIS-assisted paths are modeled using a Rician fading channel with K factor equal to 10. Although the RIS is able to assist multiple E2E paths for each UE simultaneously, the achievable gain is heterogeneous across different paths due to distance-dependent propagation and the common use of phase-shift configuration within each block. To facilitate a clear ablation study of RIS assistance more distinguishable, the RIS is deployed close to BS 1. In this deployment, the RIS phase shifts are configured to provide constructive signal combining for the overall network rather than being dedicated to a specific BS-UE pair. As a result of the geometric proximity between the RIS and BS 1, Path 1 naturally experiences more pronounced RIS-assisted gains for the BS 1-UE 1 radio link compared with other BSs. Meanwhile, UE 2 and UE 3 are placed closer to BS 2 and BS 3, respectively, resulting in different dominant access paths.

TABLE I: Main Simulation Parameters.

Parameter	Value	Parameter	Value
Traffic types q	{1, 2}	Packet size M_q (bytes)	T1: 10000 T2: 20000
Arrival rate $\lambda_{n,q}$ (pkts/s)	T1: 50 T2: 10	Latency budget T_q^{\max} (s)	T1: 0.9 T2: 1.0
Noise PSD N_0 (dBm/Hz)	-174	Carrier frequency f_c (GHz)	2.6
Total bandwidth B_{tot} (MHz)	100	Uplink transmit power P_{tot} (dBm)	23
Pathloss model	UMa NLoS [14]	UE speed(m/s)	1
Block duration t_s (ms)	50	Simulation time T_{sim} (s)	500
GBR Path 1 Q_1 (Mb/s)	T1: [100,150] T2: [180,220]	GBR Path 2 Q_2 (Mb/s)	T1: [110,140] T2: [190,200]
GBR Path 3 Q_3 (Mb/s)	T1: [105,130] T2: [170,210]	RIS location (m)	(50,86,6,20)
BS location(m)	(0,0,25); (433,0,25); (216.5,375,25)	UE location (m)	(151.6,93.8,1.8); (368.1,156.3,1.8); (66.5,318.8,1.8)
CPU	Intel Core i7 @ 2.6 GHz		

The main simulation setup is summarized in Table I, where the two traffic types have different latency budget characteristics. We further propose three baselines for comparison:

- **Single-path (SP):** Each UE transmits all traffic through a fixed access path for all traffic in all blocks.
- **Path-selection (PS):** Each UE dynamically selects a better single E2E path in each block and transmits all traffic through the selected path.
- **Multi-path (MP) without RIS:** Each UE optimally splits its traffic across all available E2E paths using the approach in prior work [1], without the RIS assistance.

We first analyze the performance gain of each UE in the system. Fig. 2 shows the cumulative distribution function (CDF) of the instant E2E latency per block for the two traffic types with different approaches. For UE 1 in Fig. 2(a), the RIS-assisted MP scheme consistently exhibits a left-shifted CDF, indicating the lower instant E2E multi-path latency in most blocks compared with other baselines. Specifically, the average E2E latency for UE 1 using the MP without RIS is 16.82 ms

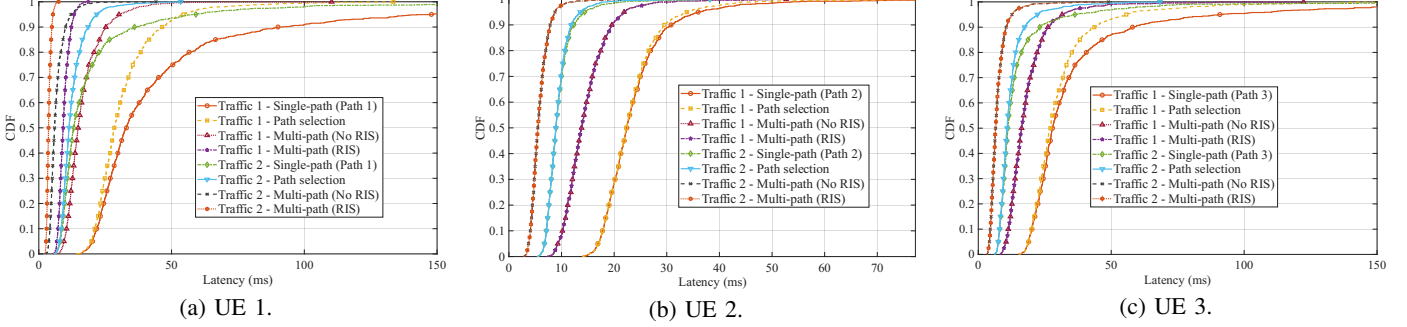


Fig. 2: The CDF of Instant E2E Latency per Block for Each UE.

and 6.72 ms for Traffic 1 and 2, respectively, which are reduced to 9.49 ms and 3.79 ms when the RIS is enabled with latency reduction of 43.56% and 43.58%. Note that the SP exhibits a pronounced long-tail behavior due to the severe radio links in some blocks. Due to the geometric proximity between the RIS, BS 1, and UE 1, the RIS-assisted multi-path scheme exhibits a more noticeable left shift in Fig. 2(a). In contrast, for UE 2 and UE 3 shown in Fig. 2(b) and (c), the latency curves of the MP with and without RIS almost overlap, indicating that the performance gain with RIS becomes weak when the RIS is too far away from the UE or the BS in the proposed system architecture.

TABLE II: Average E2E Latency (ms) per Traffic Type.

Traffic	MP with RIS (Ours)	MP [1]	SP	PS
1	14.145	16.587	39.766	28.786
2	5.653	6.630	15.896	11.506

We further investigate the performance gain of the whole system based on \bar{U} in Eq.(20). We track the average E2E latency of traffic 1 and 2 respectively, which are summarized in Table II. The MP achieves the lower average latency than both SP and PS for the two traffic types. Moreover, enabling the RIS for MP can further reduce the average E2E latency, confirming the effectiveness of RIS. Specifically, the MP with RIS reduces the average E2E latency by approximately 14.8% for Traffic 1 and 14.7% for Traffic 2, compared with the MP without RIS. In addition, compared with the SP, the MP with RIS reduces the average E2E latency up to 64% for both Traffic 1 and 2. Overall, the numerical results demonstrate that while the E2E multi-path architecture is the key factor in reducing the E2E latency, the RIS is also able to primarily provide additional performance gain especially when more favorable RIS-assisted radio links are present, leading to an around 15% performance gain in the investigated scenario.

V. CONCLUSION

This paper proposed a RIS-assisted E2E multi-path UL transmission optimization approach to achieve the minimum average E2E latency that accounts for wireless and backhaul delays for 6G time-sensitive services. We formulate an optimization problem by jointly optimizing the UL traffic-splitting ratio, UL transmit power, receive combining vector, and RIS phase shift. An alternating optimization approach combining with the SCA and SDR approaches is then developed to solve

the non-convex problem. Finally, the numerical results from simulation demonstrate that the proposed E2E MP architecture outperforms the baselines such as SP and PS schemes, meanwhile, the RIS aided for MP yields further gains by lowering the average E2E latency up to 43% for a single user and 15% for the whole system, which supports the UL transmission of 6G time-sensitive services with more stringent QoS requirements.

REFERENCES

- [1] L. Cao, A. Kiani, A. Xiang, K. John, T. Saboorian, and L. Zhang, “Latency-aware E2E multi-path data transmission optimization towards next-gen mobile networks,” in *2025 IEEE/CIC International Conference on Communications in China (ICCC Workshops)*. IEEE, 2025, pp. 1–5.
- [2] 3GPP, “Study on scenarios and requirements for next generation access technologies,” The 3rd Generation Partnership Project, Tech. Rep. TR38.913, Oct. 2025.
- [3] —, “Study on enhancement of Ultra-Reliable Low-Latency Communication (URLLC) support in the 5G Core network (5GC),” The 3rd Generation Partnership Project, Tech. Rep. TR23.725, Jun. 2019.
- [4] X. Ba, L. Jin, Z. Li, J. Du, and S. Li, “Multiservice-based traffic scheduling for 5G access traffic steering, switching and splitting,” *Sensors*, vol. 22, no. 9, p. 3285, 2022.
- [5] P. Hurtig, K.-J. Grinemo, A. Brunstrom, S. Ferlin, Ö. Alay, and N. Kuhn, “Low-latency scheduling in MPTCP,” *IEEE/ACM Transactions on Networking*, vol. 27, no. 1, pp. 302–315, 2018.
- [6] G. Zhao, Y. Li, C. Xu, Z. Han, Y. Xing, and S. Yu, “Joint power control and channel allocation for interference mitigation based on reinforcement learning,” *IEEE Access*, vol. 7, pp. 177254–177265, 2019.
- [7] Q. Wu, S. Zhang, B. Zheng, C. You, and R. Zhang, “Intelligent reflecting surface-aided wireless communications: A tutorial,” *IEEE Transactions on Communications*, vol. 69, no. 5, pp. 3313–3351, 2021.
- [8] K. Shafique and M. Alhassoun, “Going beyond a simple RIS: Trends and techniques paving the path of future ris,” *IEEE Open Journal of Antennas and Propagation*, vol. 5, no. 2, pp. 256–276, 2024.
- [9] Z. Zhu, Z. Li, Z. Chu, Y. Guan, Q. Wu, P. Xiao, M. Di Renzo, and I. Lee, “Intelligent reflecting surface assisted mmwave integrated sensing and communication systems,” *IEEE Internet of Things Journal*, vol. 11, no. 18, pp. 29427–29437, 2024.
- [10] E. Shi, J. Zhang, H. Du, B. Ai, C. Yuen, D. Niyato, K. B. Letaief, and X. Shen, “Ris-aided cell-free massive mimo systems for 6G: Fundamentals, system design, and applications,” *Proceedings of the IEEE*, vol. 112, no. 4, pp. 331–364, 2024.
- [11] G. Hu, Q. Wu, D. Xu, K. Xu, J. Si, Y. Cai, and N. Al-Dhahir, “Intelligent reflecting surface-aided wireless communication with movable elements,” *IEEE Wireless Communications Letters*, vol. 13, no. 4, pp. 1173–1177, 2024.
- [12] G. Scutari and Y. Sun, “Parallel and distributed successive convex approximation methods for big-data optimization,” in *Multi-Agent Optimization: Cetraro, Italy 2014*. Springer, 2018, pp. 141–308.
- [13] Q. Wu and R. Zhang, “Intelligent reflecting surface enhanced wireless network via joint active and passive beamforming,” *IEEE Transactions on Wireless Communications*, vol. 18, no. 11, pp. 5394–5409, 2019.
- [14] 3GPP, “Study on channel model for frequencies from 0.5 to 100 GHz,” The 3rd Generation Partnership Project, Tech. Rep. TS38.901, Mar. 2024.